

Effect of misfit dislocation on surface diffusionMaral Aminpour,^{1,*} Oleg Trushin,^{2,†} and Talat S. Rahman^{1,‡}¹*Department of Physics, University of Central Florida, Orlando, Florida 32816, USA*²*Yaroslavl Branch of the Institute of Physics and Technology of Russian Academy of Sciences, Yaroslavl, Russia*

(Received 14 December 2010; published 29 July 2011)

We apply molecular dynamics and molecular static methods to study the effect of misfit dislocations on adatom diffusion in close proximity to the dislocation core in heteroepitaxial systems, using many-body interaction potentials. Our system consists of several layers (three–seven) of Cu on top of a Ni(111) substrate. The misfit dislocations are created with the core located at the interface between the Cu film and the Ni substrate, using the repulsive biased potential method described earlier. We find that presence of the defect under the surface strongly affects the adatom trajectory, creating anisotropy in atomic diffusion, independent of the thickness of the Cu film. We also calculate the potential energy surface available to the adatom and compare the energy barriers for adatom diffusion in the proximity of the core region and on the defect-free surface.

DOI: [10.1103/PhysRevB.84.035455](https://doi.org/10.1103/PhysRevB.84.035455)

PACS number(s): 68.35.Fx, 68.43.Jk, 68.55.Ln, 68.37.—d

I. INTRODUCTION

Modern microelectronic technology depends on the ability to control the growth of thin films. Because a key factor in thin-film growth is surface diffusion,¹ a great deal of effort has been devoted to devising realistic models of this process. Many studies have focused on the effects of surface strain on diffusivity, a few on inhomogeneous^{2,3} but most on homogenous stress fields,^{4–6} and all considering only surfaces free of dislocations. Any realistic material, however, is found to be characterized by certain density of dislocations and related defects, when serving as a substrate for film growth. In heteroepitaxial growth, for example, the first few deposited layers grow pseudomorphically (following the substrate geometry) until the strain due to the lattice mismatch is released at a critical thickness leading to the formation of misfit dislocations.^{7–9} In several works^{10–13} the formation of such misfit dislocations for heteroepitaxial Lennard-Jones systems was documented using molecular static calculations of system energetics and activation energy barriers coupled with either off-lattice kinetic Monte Carlo simulations^{10–12} or application of spherical repulsive potentials¹³ to activate the nucleation process. More recently, Trushin *et al.*¹⁴ applied semiempirical interaction potentials from the embedded atom method (EAM)¹⁵ to generate misfit dislocation in heteroepitaxial growth of Pd/Cu(100) and Cu/Pd(100). As expected, the presence of misfit dislocations is found to have consequences for growth patterns through the transformation of the potential energy surface for the diffusion of the deposited atoms and their clusters.^{2,13} To our knowledge, a systematic study that documents the effect of inhomogeneous strain in modifying the diffusion dynamics of adatoms, via hopping, on heteroepitaxial systems with well-defined misfit dislocations, has not yet been carried out. To do so, we need to focus on a heteroepitaxial system, the lattice mismatch of which generates stress that is eventually released through a defect, i.e., misfit dislocation network.^{16,17} One interesting prototype system is that of Cu layers on Ni(111). We are interested first in creation of a misfit dislocation in this system for several thicknesses of the Cu film. The further purpose of this paper is to study the effects of isolated defects upon the diffusion of a Cu adatom on Cu layers on Ni(111). The stated system is of more

general interest because Cu thin films on Ni surfaces provide an interface that is of particular interest in circuit interconnects for magnetic devices exploiting the giant magnetoresistance (GMR) effect¹⁸ and for sensor systems.¹⁹ Understanding the microscopic mechanisms of thin-film growth in this system may help open up avenues for designing heteroepitaxial systems in ways that are useful for modern microelectronic technology. For example, the dislocation network, created on deposition of Ag films on Pt(111), was recently shown to guide the formation of well-ordered molecular nanostructure which may have technological applications.²⁰ In an earlier study²¹ self-organized growth of nanostructured Fe islands were observed on a dislocation network formed by a Cu bilayer on Pt(111). Such confined nanostructures may exhibit anomalous magnetic properties and thus continue to be the subject of investigation.²²

The rest of the paper is organized as follows: Section II discusses the model system and computational details. Section III elaborates on the potential energy surface available to the adatom. In Sec. IV, results of molecular dynamics (MD) simulation of the Cu adatom diffusion on the Cu/Ni(111) surface are presented. Calculated energy barriers for adatom diffusion are summarized in Sec. V, followed by conclusions in Sec. VI.

II. CONSTRUCTION OF THE MODEL SYSTEM AND COMPUTATIONAL DETAILS

Our model system consists of a Cu adatom on top of the Cu/Ni(111) substrate with an isolated misfit dislocation located at the Cu-Ni interface as presented in Fig. 1. A Cu/Ni(111) system is characterized by 2.6% lattice misfit between Cu ($a = 3.61 \text{ \AA}$) and Ni ($a = 3.58 \text{ \AA}$), which puts the Cu film under a compressive stress. The Ni(111) part of the system consists of seven layers with 250 atoms in a layer, on top of which three, five, or seven layers of Cu atoms are placed. Since the results for both molecular dynamics (MD) simulations and molecular static (MS) calculations for the activation energy barriers turned out to be the same, regardless of whether the Cu film in the model was three, five, or seven layers thick, we will confine our illustrations in what follows to the five-layer case. We set periodic boundary conditions in

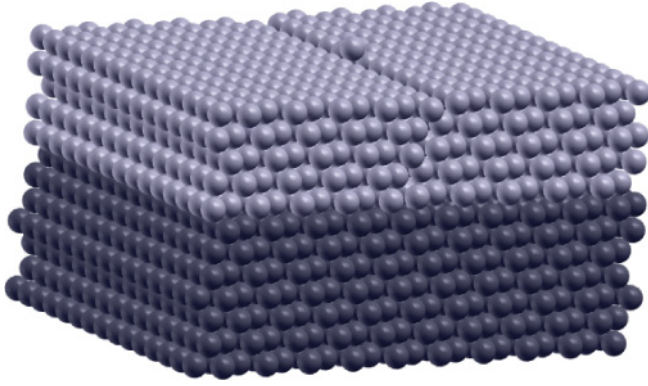


FIG. 1. (Color online) A Cu adatom on the dislocated surface of a five-layer Cu film on a Ni(111) substrate.

the plane parallel to the substrate surface in such a way as to mimic an infinitively large system.

Furthermore, to introduce an ideal misfit dislocation into our sample, we used a procedure called the repulsive biased potential (RBP) method described in detail elsewhere,^{13,14} which allows one to activate the transition of many atomic systems from the coherent state (without defect) to the relaxed state (with defect). In this approach, the system is first relaxed through MD cooling²³ in which the energy is gradually minimized by setting each particle velocity to zero whenever it has a component opposite to the direction of the acceleration. New positions and velocities are calculated through the standard leap-frog algorithm. This leads to an initial coherent epitaxial state in which the interlayer spacing is relaxed, but atoms within the layers are under compressive stress according to the misfit [see Fig. 2(a)]. Next, a repulsive biased potential is applied¹³ to the system by adding an exponentially decaying spherically symmetric potential to the original potential energy surface. The latter is sufficiently localized around the initial harmonic basin to ensure that the final-state energy does not depend upon the artificially applied repulsive bias, but solely upon the true potential of the system. The main idea here is to modify the local energy surface such that the initial epitaxial state becomes unstable. Following this, the system is slightly displaced from the metastable state (randomly or in a selective way to escape from the harmonic basin) and the total energy minimization procedure is applied to find a new minimum energy state. As a result, a rectangular island of atoms protrudes onto the surface, leaving a dislocation underneath. This method can generate many different final states depending on both the initial displacements and the parameters of the repulsive potential. Here, we only consider final configurations corresponding to a single misfit dislocation. The width of the (two-dimensional) island that is created corresponds exactly to the thickness of the film [for instance, the five-atom island is seen in Fig. 2(b)]. In the third phase of defect activation, this extended island is manually removed, resulting in a surface with a defect extending through the thickness of the film as seen in the Fig. 2(c). It should be mentioned that our method of producing a single misfit dislocation is quite robust. We have repeated the procedure several times and found convergence by considering the net force acting on an atom to be less than

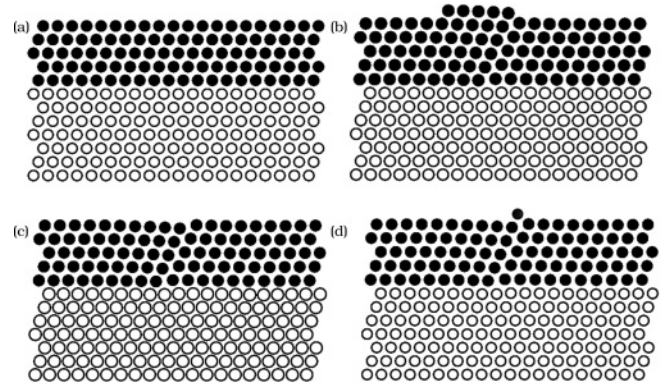


FIG. 2. Schematic (two-dimensional) representation of the procedure for preparing a sample consisting of a five-layer film on a seven-layer substrate: (a) relaxation of the sample using standard MD cooling energy minimization; (b) formation of a protruded island, resulting from application of RBP, followed by a second phase of MD cooling; (c) removal of the island and visible appearance of the underlying dislocation; (d) addition of a single Cu adatom on top of the film. (In the study we vary the position of this adatom with respect to the defect).

10^{-6} eV/Å. We have also checked this by comparing our results with that obtained by others.²⁴

The presence of the defect inside the substrate generates an inhomogeneous strain field on the surface. To study the effect of this field on the kinetics of diffusion, we place a single Cu adatom at various positions on the film surface near the defect. We probe the influence of this stress field in three ways for both the defect-free and the dislocated surface: (1) map the binding energy of the adatom with respect to each position within a fine grid on the surface of the film, (2) perform direct MD simulations of the adatom diffusion from selected initial positions on the film, and (3) for each of these positions, calculate the diffusion barrier for paths perpendicular and parallel to the dislocation line.

To prevent the motion of the system as a whole, we fixed the two bottom layers of the Ni substrate. In MD calculations, we used the leap-frog algorithm with a time step of 1 fs (10^{-15} s) to solve classical equations of motion for atoms interacting through interatomic potentials given by the embedded atom method (EAM).¹⁵ We carried out simulations at 300 K using the canonical ensemble. To monitor the overall trajectory of the adatom diffusing from a given initial position, we ran each simulation for 1 ns (10^{-9} s), recording statistics every 10 time steps. We used the nudged elastic band (NEB) method²³ to calculate all activation energy barriers. Typically, the path in configuration space is modeled by 20 discrete states or images. Forces on the images converged to better than 10^{-6} eV/Å.

III. MAPPING THE POTENTIAL ENERGY SURFACE OF THE ADATOM

To see how the presence of the defect under the substrate surface modifies the potential energy experienced by the adatom at different locations on the film, we compared the energy maps of the potential energy surface of our sample with and without dislocation. To obtain each map we scanned the surface by placing the adatom at different positions on a

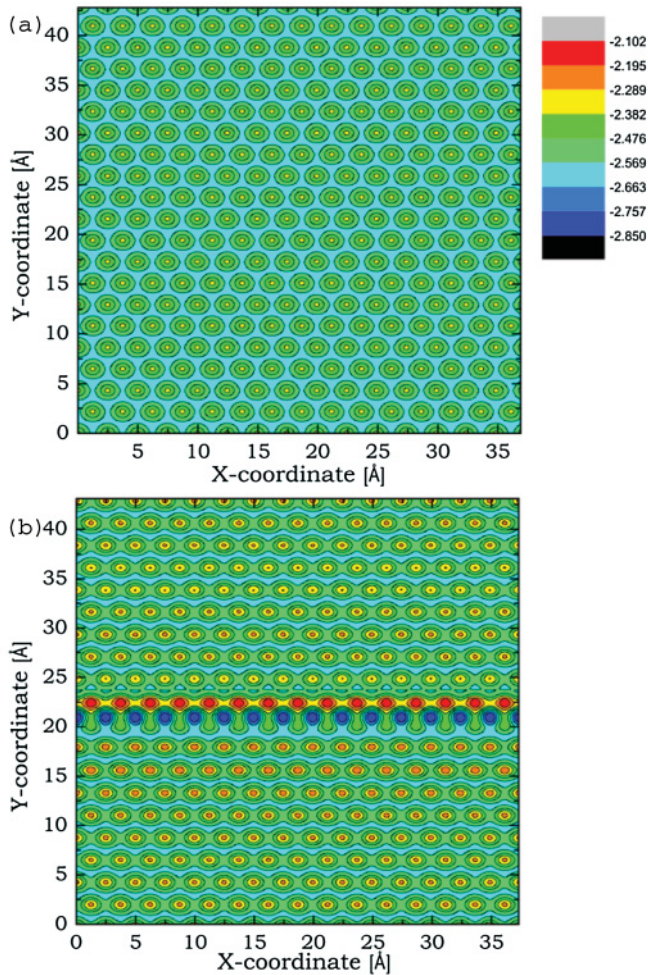


FIG. 3. (Color online) Potential energy surface for the (a) defect-free surface and (b) dislocated surface.

fine grid ($0.1 \times 0.1 \text{ \AA}$) covering a wide area of the film surface. At each site of the grid, we fixed the X and Y coordinates of the adatom and left the Z coordinate free to relax, and then used MD cooling to minimize the system energy. The resulting energy map shows the binding sites of the adatom on the surface of the film, as shown in Figs. 3(a) and 3(b) for the ideal coherent substrate (i.e., without defect) and for the substrate with a defect inside it, respectively. Clearly the presence of the defect beneath the film surface alters the binding energy map of the adatoms to the surface. The isotropy of the surface vanishes in favor of trap zones (very deep minima) along the dislocation line, which can immobilize any adatom that strays into its vicinity during a random walk across the surface.

IV. MD SIMULATIONS OF ADATOM DIFFUSION ON Cu FILM ON Ni(111)

Another way to probe the effect of the defect on surface diffusion is direct MD simulation of adatom motion on the surface. Although intrinsic limitations of the MD method do not allow documentation of trajectories for the adatoms for times comparable to experiments (runs of a few nanoseconds), the statistics afforded by us do reveal some insights into how the presence of a defect imposes a specific form of

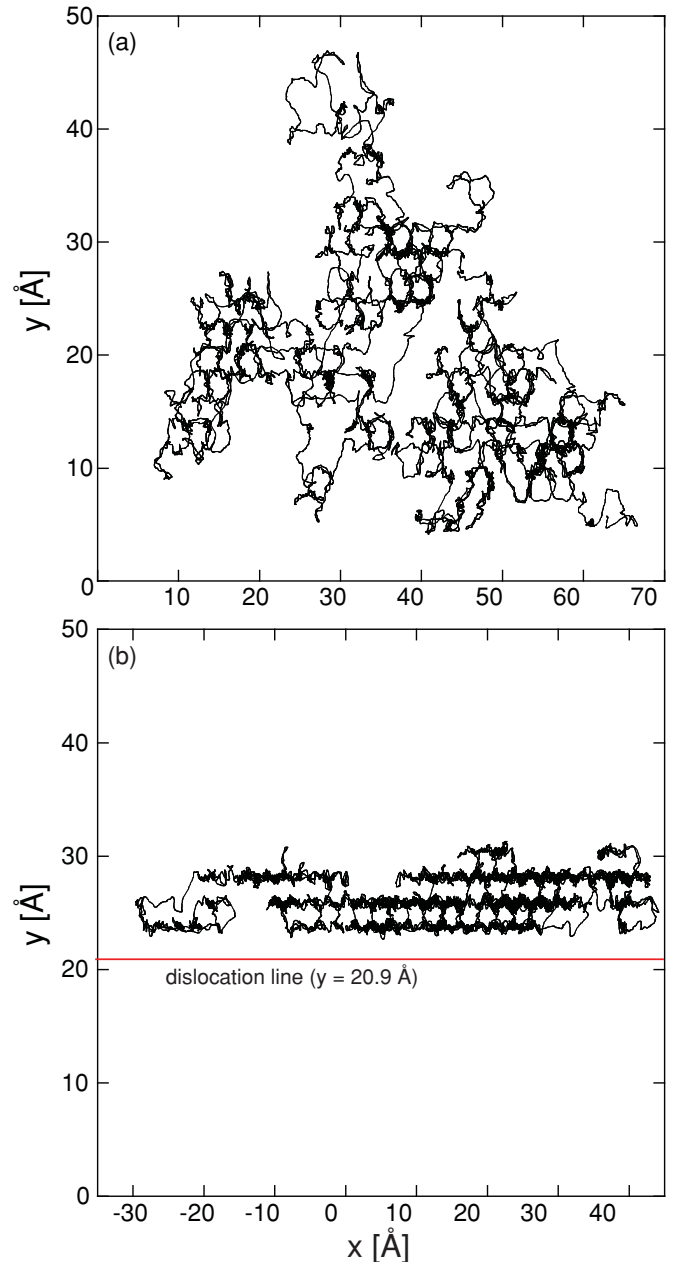


FIG. 4. (Color online) (a) A typical isotropic trajectory of the adatom on a defect-free surface. (b) A typical anisotropic trajectory of the adatom on a defective surface when its initial position is one-row distant from the dislocation line, which runs parallel to the edge of the slab 26 \AA from it.

organization upon what would otherwise be a random walk. If we compare a typical trajectory of adatom motion on the ideal surface [Fig. 4(a)] with that on a dislocated surface [Fig. 4(b)], the anisotropy of the latter is obvious. The starting point of the simulations traced in Fig. 4(b) is one row from the dislocation line. Since all the way to the slab edge we find the same anisotropy, we can infer that the strain field due to isolated edge dislocation extends far beyond the dislocation core. Close to the dislocation line, we observe a different kind of strain effect: trap zones form along the dislocation line, limiting diffusion in striking ways. If we place the adatom directly

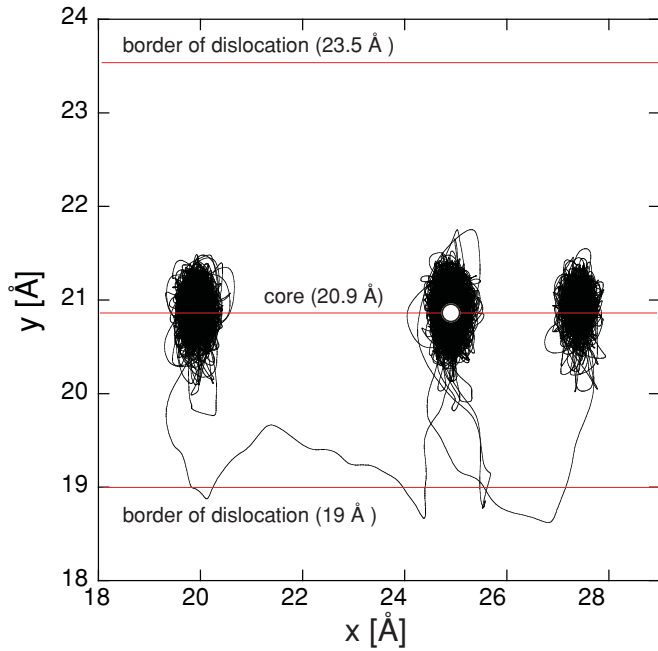


FIG. 5. (Color online) Trajectory from MD simulations of attachment and detachment of adatom along dislocation line. (Starting point is 21 Å away from the edge of the slab.) The white dot is the starting point of the simulation.

on the dislocation line it almost always exhibits a severely confined (spot-bound) trajectory. Although escapes do occur, they are extremely rare; usually when an adatom wanders from its initial position, it shortly returns, and continues to hover around it. Sometimes the escape extends as far as one row from the dislocation, in which case it exhibits an anisotropic trajectory [like that in Fig. 4(b)]. On others, after dwelling in the neighborhood of its initial position, it can escape a short distance toward the border and then return to the dislocation core but at a position on the core at some lateral distance in either direction from its initial zone of entrapment (see Fig. 5).

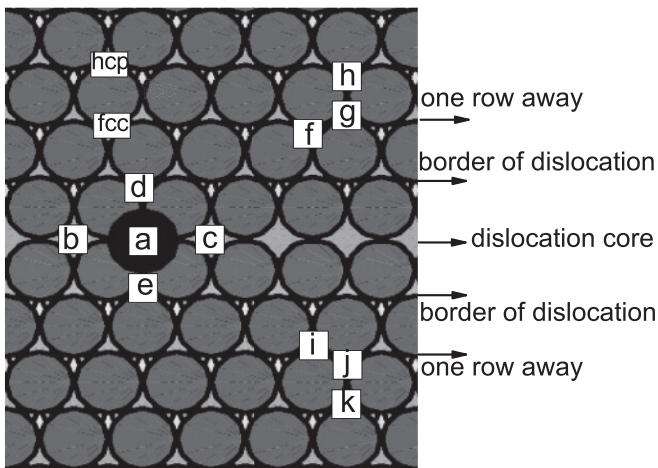


FIG. 6. (Color online) Locations of the adatom on the dislocated surface.

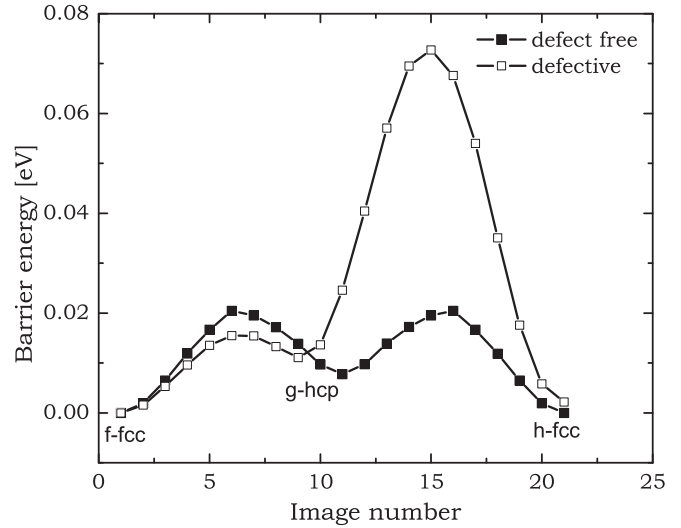


FIG. 7. Energy barriers on a (a) defect-free and (b) defective surface for a diffusion path from an fcc (f) to an fcc (h) site by way of an hcp (g) site (f, g, and h sites are shown in Fig. 6). For the defective surface, the higher barrier corresponds to the motion in the direction perpendicular to the dislocation line.

V. ENERGY BARRIERS FOR ADATOM DIFFUSION PROCESSES

To further pin down the effect of the submerged defect on surface diffusion, we calculated the energy barriers for the adatom to diffuse via hopping along possible paths both on the defect-free substrate and on the defective one. We graph the energy barriers for an adatom’s diffusion along its path from an fcc to an fcc site by way of an hcp site on both the defect-free surface and the defective surface (Fig. 7). Let us consider such a diffusion path. On both surfaces the path consists of two steps: the first from the initial fcc site to an hcp site, and the second from there to the other fcc site. On the defective surface (see Fig. 6), for an adatom one row away from the border of the dislocation, the first step (f→g) is “parallel” to the dislocation line (actually at an acute angle to it), while the second (g→h) is “perpendicular” to that border. On the defect-free surface, the energy barriers for the two steps (fcc→hcp and hcp→fcc) are 0.01 and 0.02 eV, respectively. Figure 7 dramatizes how the saddle points of barrier energy for diffusion steps on the defect-free surface are symmetrical, while those for the equivalent steps on the defective surface are highly asymmetrical: the barrier for the step perpendicular to the dislocation border (g→h : 0.06 eV) is three times higher than that for the step parallel (f→g : 0.02 eV) to it, reminding us of the repulsive barriers for adatoms set up by the dislocation network mentioned in Ref. 21. The difference explains the contrast between anisotropic diffusion trajectories typical on the defective surface [Fig. 4(b)] and the isotropic trajectories typical on the defect-free surface [Fig. 4(a)]. The same asymmetrical behavior is obtained for the perpendicular (j→k : 0.09 eV) and the parallel (i→j : 0.03 eV) paths in Fig. 6.

We turn now to the diffusion of an adatom located in the core of the dislocation. The barrier for diffusion in either direction within the dislocation core (a→c and a→b) is 0.42 eV. The barriers for diffusion away from the core are 0.5 eV for a→d

and 0.23 for $a \rightarrow e$. The barriers for an adatom at the core border to be trapped in the core are 0.22 eV ($d \rightarrow a$) and 0.0 ($e \rightarrow a$). Thus there is a very strong tendency for an adatom situated in the core to stay where it is, and not to move away from or along the dislocation. We thus expect that the atom will only very rarely move along the dislocation line. Instead it will stay for some time in the trap zone. Because the trapping barrier is smaller than the escaping barrier, we would expect to see from time to time—as we did in our MD simulations (Fig. 5)—a detachment followed by either a return to the original zone of entrapment or a fall into a neighboring entrapment zone. One point to note is that sometimes movement from one entrapment zone to a neighboring one occurs via a trip to the dislocation border. Moreover, if an adatom occupies a border site, it can wander even farther, to a position one row away from the dislocation. Once it reaches this distance from the dislocation core, it behaves in virtually the same way as an adatom at any farther distance, and its trajectory will exhibit the kind of anisotropic pattern illustrated in Fig. 4(b).

VI. CONCLUSIONS

We compared the diffusion of a Cu adatom on the dislocation surface of a heteroepitaxial Cu/Ni(111) substrate with its diffusion on the same substrate in which dislocation is left out of account. Mapping of the potential energy surface, MD simulations of adatom trajectories, and calculation of activation energies for single adatom diffusion paths indicate

that the presence of a defect within the substrate profoundly affects surface diffusion. The strain field produced by isolated edge dislocation extends a long way (at least six rows, i.e., to the end of the unit cell under study) from the dislocation core, on both sides. Diffusion at one or more rows away from the dislocation border is anisotropic and symmetrical on both sides of the dislocation, in contrast to the isotropic trajectory that emerges on a defect-free surface. At the dislocation core, entrapment zones appear, from which an adatom is highly unlikely to escape. On the other hand, if adatoms appear a row or so away from the border of dislocation, they stay repelled from it. We thus expect adatoms to nucleate either at the dislocation core (trapped) or in regions farther away from them. In either case, the growth pattern on surfaces such as the ones considered here will be reflective of a dislocation network. We note that such surface nanostructuring induced by a dislocation network has already been observed experimentally.^{20,21} We hope that our work will motivate more experimental research in the area. Of course, additional diffusion processes have to be considered if one aims at the study of multilayer growth on dislocation networks.

ACKNOWLEDGMENTS

We are indebted to Lyman Baker and Giridhar Nandipati for insightful discussions and numerous helpful suggestions during the preparation of this manuscript. The work was supported in part by US-NSF under Grant No. 0840389.

*maral@knights.ucf.edu

†oleg_trushin@lenta.ru

‡Talat.Rahman@ucf.edu

¹T. Ala-Nissila, R. Ferrando, and S. C. Ying, *Adv. Phys.* **51**, 949 (2002).

²M. Schroeder and D. E. Wolf, *Surf. Sci.* **375**, 129 (1997).

³C. Goyhenex, K. Farah, and A. Taobane, *Surf. Sci.* **601**, L132 (2007).

⁴H. Brune, K. Bromann, H. Röder, K. Kern, J. Jacobsen, P. Stoltze, K. Jacobsen, and J. Nørskov, *Phys. Rev. B* **52**, 14380(R) (1995).

⁵C. Ratsch and M. Scheffler, *Phys. Rev. B* **58**, 13163 (1998).

⁶W. Xiao, P. A. Greaney, and D. C. Chrzan, *Phys. Rev. Lett.* **90**, 156102 (2003); *Phys. Rev. B* **70**, 033402 (2004).

⁷J. C. Bean, *Science* **230**, 127 (1985).

⁸C. A. B. Ball and J. H. van der Merwe, in *Dislocation in Solids*, edited by F. R. N. Nabarro (North-Holland, Amsterdam, 1983).

⁹J. W. Matthews and A. E. Blakeslee, *J. Cryst. Growth* **27**, 118 (1974).

¹⁰F. Much and M. Biehl, *Europhys. Lett.* **63**, 14 (2003).

¹¹T. Volkman, F. Much, M. Biehl, and M. Kotrla, *Surf. Sci.* **586**, 157 (2005).

¹²M. Walther, M. Biehl, and W. Kinzel, *Phys. Status Solidi C* **4**, 3210 (2007).

¹³O. Trushin, E. Granato, S.-C. Ying, P. Salo, and T. Ala-Nissila, *Phys. Rev. B* **65**, 241408(R) (2002).

¹⁴O. Trushin, J. Jalkanen, E. Granato, S. C. Ying, and T. Ala Nissila, *J. Phys. Condens. Matter* **21**, 084211 (2009).

¹⁵S. M. Foiles, M. I. Baskes, and M. S. Daw, *Phys. Rev. B* **33**, 7983 (1986).

¹⁶S. A. Campbell, *The Science and Engineering of Microelectronic Fabrication* (Oxford University, Oxford, 1996), p. 341.

¹⁷H. Luth, *Surfaces and Interfaces of Solid Materials* (Springer-Verlag, Berlin, 1995).

¹⁸C. A. Chang, *J. Vac. Sci. Technol. A* **3779**, (1990).

¹⁹S. Semancik, R. E. Cavicchi, K. G. Kreider, J. S. Suehle, and P. Choparala, *Sens. Actuators B* **34**, 209 (1996).

²⁰K. Ait-Mansour, M. Treier, P. Rufeux, M. Bieri, R. Jaafar, P. Groning, R. Fasel, and O. Groning, *J. Phys. Chem. C* **113**, 8407 (2009).

²¹H. Brune, M. Giovannini, K. Bromann, and K. Kern, *Nature (London)* **394**, 451 (1998).

²²E. D. Tober, R. F. Marks, D. D. Chambliss, K. P. Roche, F. M. Toney, A. J. Kellock, and R. F. C. Farrow, *Appl. Phys. Lett.* **77**, 2728 (2000).

²³H. Jónsson, G. Mills, and K. W. Jacobsen *Classical and Quantum Dynamics in Condensed Phase Simulations*, edited by B. J. Berne et al. (World Scientific, Singapore, 1998).

²⁴V. Bulatov and W. Cai, *Computer Simulations of Dislocations*, (Oxford University, Oxford, 2006), Chap. 4.